Synthesis, structural studies and Hirshfeld surface analysis of 2-[(4-phenyl-1H-1,2,3-triazol-1-yl)methyl]pyridin-1-ium hexakis(nitrato-$\kappa^2 O,O'$)thorate(IV)

Shalini Rangarajan,[a,b] Sonu Sheokand,[b] Victoria L. Blair,[c] Glen B. Deacon[c] and Maravanji S. Balakrishna[b]*

[a]IITB-Monash Research Academy, Indian Institute of Technology Bombay, Mumbai 400076, India, [b]Phosphorus Laboratory, Department of Chemistry, Indian Institute of Technology, Bombay, Mumbai 400076, India, and [c]School of Chemistry, Monash University, Melbourne Clayton, Victoria 3800, Australia. *Correspondence e-mail: krishna@chem.iitb.ac.in

Reaction of thorium(IV) nitrate with 2-[(4-phenyl-1H-1,2,3-triazol-1-yl)methyl]pyridine (L) yielded $(LH)_2[Th(NO_3)_6]$ or $(C_{14}H_{13}N_4)_2[Th(NO_3)_6]$ (1), instead of the expected mixed-ligand complex $[Th(NO_3)_4L_2]$, which was detected in the mass spectrum of 1. In the structure, the $[Th(NO_3)_6]^{2-}$ anions display an icosahedral coordination geometry and are connected by LH^+ cations through C—H⋯O hydrogen bonds. The LH^+ cations interact via N—H⋯N hydrogen bonds. Hirshfeld surface analysis indicates that the most important interactions are O⋯H/H⋯O hydrogen-bonding interactions, which represent a 55.2% contribution.

1. Chemical context

The nitrate ion with its small chelate or bite angle has a low steric footprint and is able to stabilize high coordination numbers. Thus 12-coordinate $[Th(NO_3)_6]^{2-}$ has been isolated and structurally characterized with a variety of counter-cations such as: $phen_2H^+$ (phen = 1,10-phenanthroline; Amani & Tayebee, 2013), $bpyH_2^{2+}$ (bpy = 4,4′-bipyridine; Rammo et al., 1994) and NH_4^+ (Spirlet et al., 1992), acetylpyridinium(thiosemicarbazone) (Abram et al., 1999), 2,2′-bipyridinium (Kumar & Tuck, 1984), [5,10,15,20-tetrakis(pyridinium-4-yl)porphyrin] (Mishra et al., 2019), 1-ethyl-3-methyl-1H-imidazol-3-ium (Kelley et al., 2020), among others (see Database survey section). Other interesting complexes are bis-(oxonium dicyclohexano-18-crown-6) hexakis(nitrato-O,O′)-thorium(IV) where the counter-cation is H_3O^+ (Wang et al., 1988) and bis[trinitrato-tetrakis(trimethylphosphine oxide)thorium(IV)] hexanitratothorium(IV) (Alcock et al., 1978) where both the anion and the cation are Th^{IV} complex ions.

Hexanitratothorate $[Th(NO_3)_6]^{2-}$ and its analogous species are important in the speciation and separation of actinoid complexes in nitric acid (Zhang et al., 2017; Surbella et al., 2018; Takao et al., 2019, 2020; Reilly et al., 2012; Matonic et al., 2002; Crawford et al., 2009; Rebizant et al., 1988).
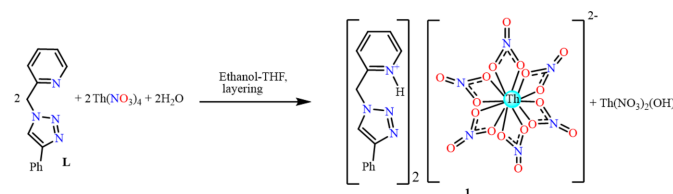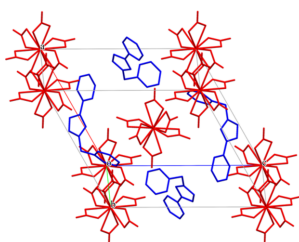
Table 1
Selected geometric parameters (Å, °).

Th1—O1	2.5830 (13)	N1—N2	1.314 (2)
Th1—O2	2.5621 (14)	N3—N2	1.343 (2)
Th1—O4	2.5583 (13)	N3—C2	1.346 (2)
Th1—O5	2.5547 (14)	N3—C3	1.461 (2)
Th1—O7	2.5444 (13)	N4—C4	1.340 (3)
Th1—O9	2.5827 (12)	N4—C8	1.351 (2)
N1—C1	1.369 (2)	N4—H4	0.862 (16)
O7—Th1—O4^i	113.48 (4)	O9^i—Th1—O1^i	66.86 (4)
O7—Th1—O4	66.52 (4)	O2^i—Th1—O9^i	112.31 (4)
O7^i—Th1—O9	130.23 (4)	O2^i—Th1—O1^i	49.70 (4)
O7—Th1—O9	49.77 (4)	O2^i—Th1—O1	130.30 (4)
O7^i—Th1—O1^i	65.87 (4)	O2—Th1—O1	49.70 (4)
O7—Th1—O2^i	69.99 (4)	O5^i—Th1—O4	130.01 (4)
O7^i—Th1—O5^i	67.80 (4)	O5—Th1—O4	49.99 (4)
O4^i—Th1—O9^i	110.18 (4)	O5^i—Th1—O9	66.29 (4)
O4^i—Th1—O1^i	112.94 (4)	O5^i—Th1—O9^i	113.71 (4)
O4^i—Th1—O2^i	113.64 (4)	O5^i—Th1—O1^i	69.63 (4)
O9—Th1—O9^i	180.0	O5^i—Th1—O2^i	67.02 (4)

Symmetry code: (i) $-x+1, -y+1, -z+1$.

Table 2
Hydrogen-bond geometry (Å, °).

D—H$\cdots A$	D—H	H$\cdots A$	$D\cdots A$	D—H$\cdots A$
N4—H4$\cdots$N1^{ii}	0.86 (3)	1.88 (3)	2.738 (3)	170 (3)
C2—H2$\cdots$O8^{iii}	0.95	2.33	3.261 (3)	168
C7—H7$\cdots$O5^{iv}	0.95	2.46	3.379 (3)	164
C13—H13$\cdots$O4^v	0.95	2.46	3.377 (3)	163
N4—H4$\cdots$N2^{ii}	0.86	2.65 (3)	3.432 (3)	151
C10—H10$\cdots$O8^{iii}	0.95	2.68	3.621 (3)	173
C5—H5$\cdots$O2^i	0.95	2.68	3.191 (2)	114
C7—H7$\cdots$O2^{iii}	0.95	2.67	3.279 (3)	123
C7—H7$\cdots$O9^{iii}	0.95	2.69	3.369 (2)	129

Symmetry codes: (i) $-x+1, -y+1, -z+1$; (ii) $-x+1, -y+1, -z+2$; (iii) $-x+\frac{3}{2}, y+\frac{1}{2}, -z+\frac{3}{2}$; (iv) $x-\frac{1}{2}, -y+\frac{1}{2}, z-\frac{1}{2}$; (v) $-x+\frac{1}{2}, y+\frac{1}{2}, -z+\frac{3}{2}$.

Reaction of Th(NO$_3$)$_4$·5H$_2$O with 2-[(4-phenyl-1H-1,2,3-triazol-1-yl)methyl]pyridine (L) resulted in the formation of the nitrato complex (LH)$_2$[Th(NO$_3$)$_6$] (**1**), instead of [Th(NO$_3$)$_4L_2$], analogous to complexes of functionalized chelating pyridine-based ligands (Gephart *et al.*, 2009; Xiao *et al.*, 2014). The structure of complex **1** was established by X-ray crystallography, IR and mass spectroscopic data.

2. Structural commentary

Compound **1** crystallized in the monoclinic $P2_1/n$ space group as a dianionic complex with two LH$^+$ pyridinium counter-cations, as shown in Fig. 1. The thorium atom is located on an inversion centre and is coordinated by six chelating nitrate ions to assume a distorted icosahedral stereochemistry (Fig. 1c), similar to other reported hexanitratothorate(IV) complexes (Abram *et al.*, 1999; Amani & Tayebee, 2013; Rammo *et al.*, 1994; Spirlet *et al.*, 1992). The Th—O bond lengths [2.5444 (13)–2.5830 (13) Å; Table 1] are similar to those reported, for example, for (H$_2$ATPSC)$_2^{2+}$-[Th(NO$_3$)$_6$]$^{2-}$·4MeOH [2.553 (3)–2.580 (3) Å; HATPSC = 2-acetylpyridine thiosemicarbazone; Abram *et al.*, 1999], (phen$_2$H$^+$)$_2^{2+}$[Th(NO$_3$)$_6$]$^{2-}$·2H$_2$O [2.555 (7)–2.572 (6) Å; Amani & Tayebee, 2013], bpyH$_2^{2+}$[Th(NO$_3$)$_6$]$^{2-}$·2H$_2$O [2.567 (17)–2.599 (16) Å; Rammo *et al.*, 1994] and (NH$_4$)$_2^{2+}$[Th(NO$_3$)$_6$]$^{2-}$ [2.545 (6)–2.608 (5) Å; Spirlet *et al.*, 1992]. The pyridine nitrogen atom of the ligand is protonated. The pyridine N—C bond lengths in **1** are N4—C8 = 1.351 (2) Å and N4—C4 = 1.340 (3) Å [1.342 (5) Å and
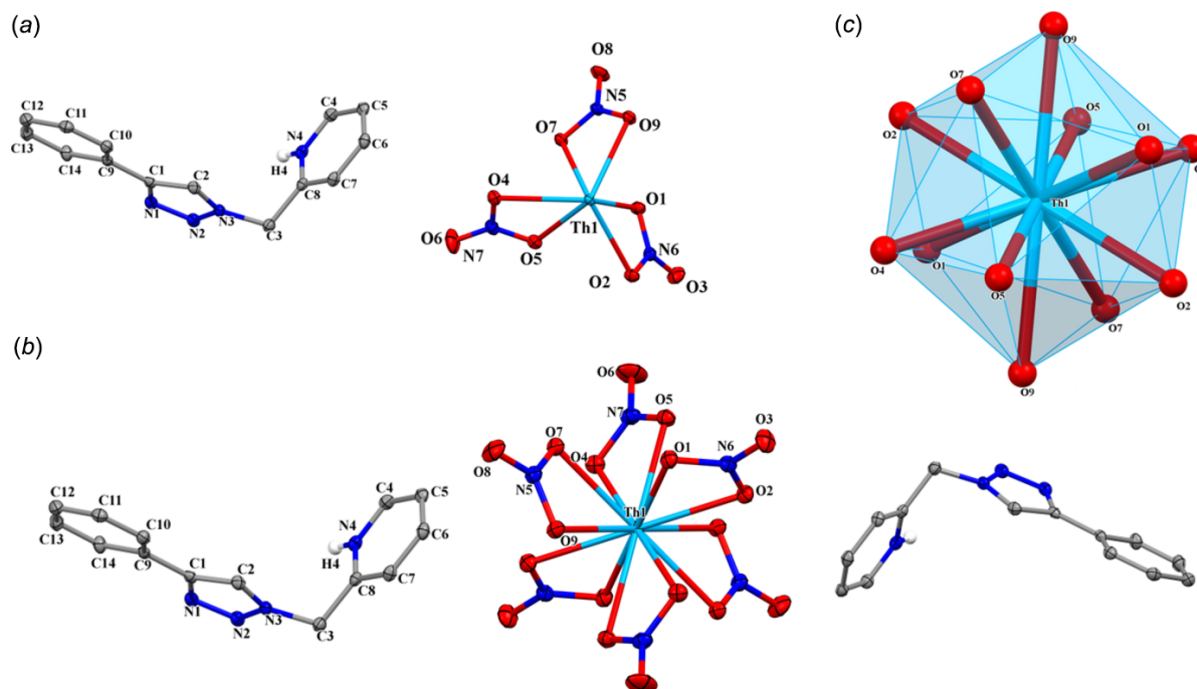

Figure 1
Molecular structure of **1**: (a) Asymmetric unit of **1** showing the atom-labelling scheme, (b) perspective view of complex **1** and (c) coordination polyhedron around the Th^{IV} atom in **1**. The hydrogen atoms are omitted for clarity except for the pyridinium hydrogen. Displacement ellipsoids are drawn at the 30% probability level.
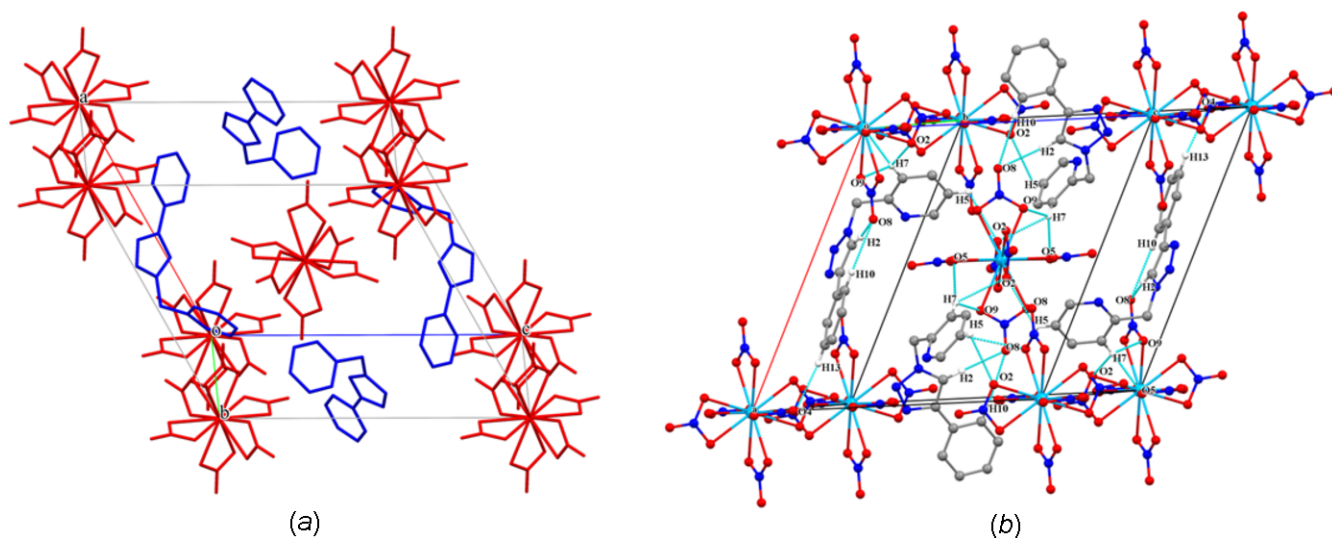
Figure 2
(*a*) The packing of complex **1** showing the $[C_{14}H_{13}N_4]^+$ cations in face-centered positions and $[Th(NO_3)_6]^{2-}$ anions at the corners and in body-centered locations and (*b*) packing diagram showing intermolecular C—H···O hydrogen-bonding interactions (blue dotted lines).

1.340 (5) Å in *L*; Urankar *et al.*, 2010] and the N4—H4 (pyridinium salt) bond distance is 0.862 (16) Å. In the triazole ring, the N—C distances are N1—C1 = 1.369 (2) Å and N3—C2 = 1.346 (2) Å [1.338 (5) and 1.353 (5) in *L*].

3. Supramolecular features and Hirshfeld Surface Analysis

In the crystal, N—H···N and C—H···O hydrogen-bonding interactions are observed (Table 2). The packing also features C—H···π(ring) [C3—H3A···Cg1($\frac{1}{2}$ + *x*, $\frac{3}{2}$ − *y*, $\frac{1}{2}$ − *z*) = 3.2029 (1) Å], π(ring)–π(ring) [Cg1···Cg2(1 − *x*, 2 − *y*, 2 − *z*) centroid–centroid distance = 3.6130 (11) Å] and O···C [N6—O3···Cg3($\frac{3}{2}$ − *x*, $\frac{1}{2}$ + *y*, $\frac{3}{2}$ − *z*) = 3.7492 (18) Å] interactions where *Cg*1, *Cg*2 and *Cg*3 are the centroids of rings C9–C14, N1–N3/C1/C2, and N4/C4–C8, respectively. A C11···H3A(−$\frac{1}{2}$ + *x*, $\frac{3}{2}$ − *y*, −$\frac{1}{2}$ + *z*) short contact of 2.69 Å also

occurs. Views of the packing of the cations and anions are displayed in Fig. 2*a* and 2*b*.

In order to visualize the intermolecular interactions in the structure of **1**, a Hirshfeld surface (HS) analysis was carried out (Spackman & Jayatilaka, 2009) and the associated two-dimensional fingerprint plots (McKinnon *et al.*, 2007) were generated using *CrystalExplorer 17.5* (Turner *et al.*, 2017). A view of the three-dimensional Hirshfeld surface plotted over d_{norm} with the red, white and blue regions indicating contacts with distances shorter, equal and longer, respectively, than the van der Waals separations (Fig. 3). Interactions between donor and acceptor atoms are seen as red spots on the Hirshfeld surface mapped over d_{norm} (Fig. 3), corresponding to C2—H2···O8, N4—H4···N1, C7—H7···O5 and C13—H13···O4 hydrogen bonds. Fig. 4 shows the overall two-dimensional fingerprint plot and and those delineated into O···H/H···O (55.2%), H···H (11.2%), N···H/H···N
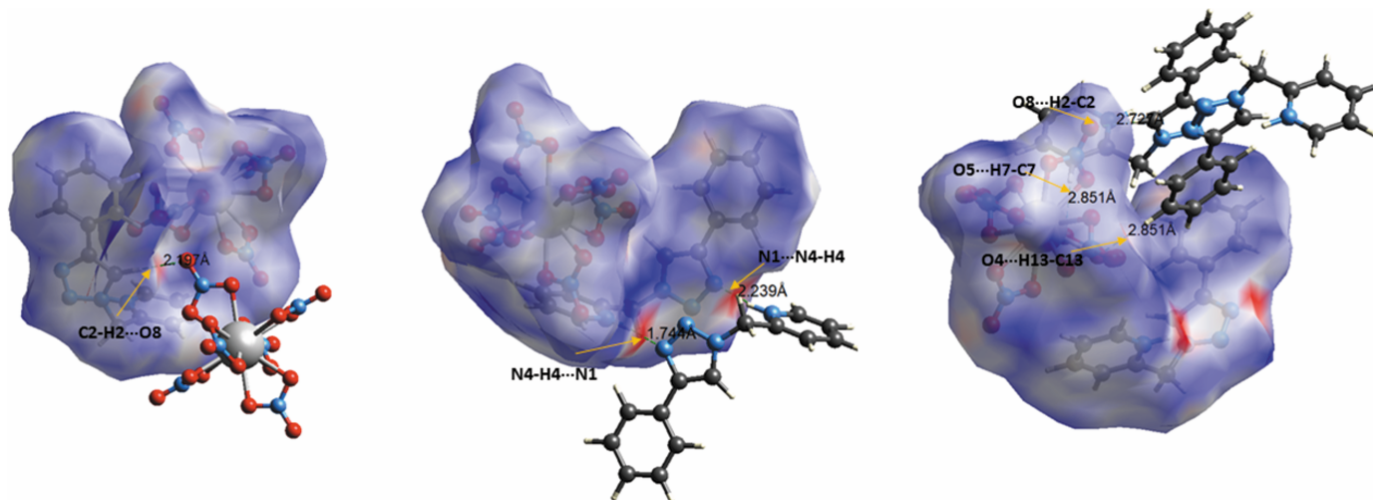

Figure 3
The three-dimensional Hirshfeld surface of the title compound **1**, plotted over d_{norm} in the range. The hydrogen bonds are shown as dashed lines.
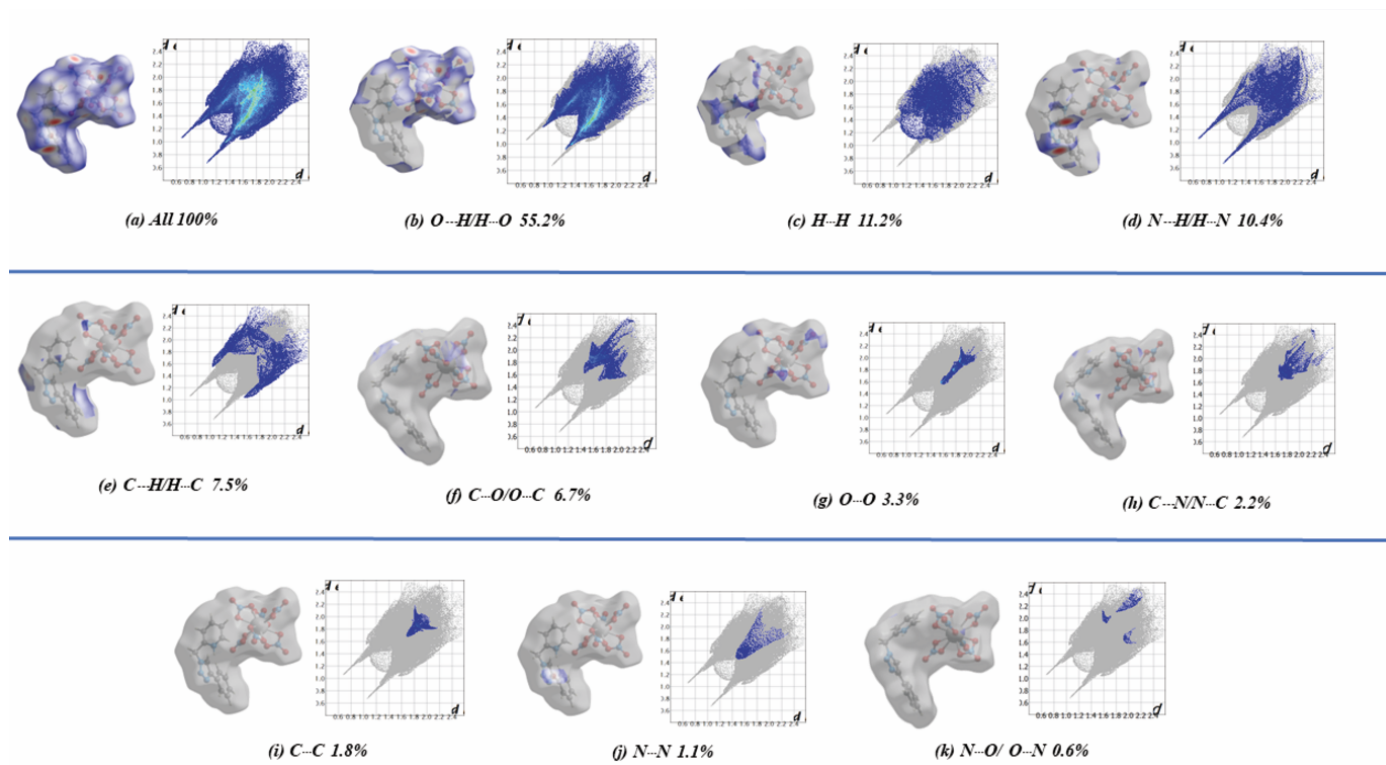
Figure 4
Hirshfeld surface of **1** mapped over d_{norm} (left images of each pair) with the corresponding two-dimensional fingerprint plots (right images of each pair). The d_i and d_e values are the closest internal and external distances (in Å) from given points on the Hirshfeld surface.

(10.4%), C···H/H···C (7.5%), C···O/O···C (6.7%), O···O (3.3%), C···N/N···C (2.2%), C···C (1.8%), N···N (1.1%) and N···O/O···N (0.6%) interactions. The large number of O···H/H···O, N···H/H···H, C···H/H···C and H···H interactions suggest that hydrogen bonding and van der Waals interactions play a major role in the crystal packing of **1**.

4. Database Survey

A search of the Cambridge Structural Database (CSD, Version 5.43, last update November 2022; Groom *et al.*, 2016) for a 12-coordinate $[Th(NO_3)_6]^{2-}$ moiety yielded several compounds related to the title compound, *viz.* CSD refcodes BEQVAU (Abram *et al.*, 1999), FERKOD (Cheng *et al.*, 2005), LEWNIM (Amani & Tayebee, 2013), YUWWAO (Rammo *et al.*, 1994), GOBTAS (Wang *et al.*, 1988), JOKRIN (Mishra *et al.*, 2019), LUDMIJ (Kelley *et al.*, 2020), NMPOTH (Alcock *et al.*, 1978), TEQVIX, TEQVUJ, TEQWEU, TEQWIY, TEQWUK, TEQXIZ, TEQXOF and ZIYCER01 (Jin *et al.*, 2017), UNAKAV (Goodgame *et al.*, 2003) and ZEWBOS (Aparna *et al.*, 1995). A search for lanthanide or actinide compounds with the ligand *L* did not return any hits.

5. Synthesis and crystallization

The ligand 2-[(4-phenyl-1*H*-1,2,3-triazol-1-yl)methyl]pyridine (*L*) was prepared as reported (Urankar *et al.*, 2010). $Th(NO_3)_4 \cdot 5H_2O$ was purchased from a local source. Infrared

spectra (4000–450 cm^{-1}) of solid samples were recorded on a Bruker Alpha II instrument using the attenuated total reflection (ATR) measurement mode. The mass spectrum was recorded using a Bruker Maxis Impact LC-q-TOF Mass Spectrometer.

A solution of 2-[(4-phenyl-1*H*-1,2,3-triazol-1-yl)methyl]pyridine (*L*) (24 mg, 0.10 mmol) in ethanol (10 ml) was layered over a solution of $Th(NO_3)_4 \cdot 5H_2O$ (57 mg, 0.10 mmol) in THF (10 ml). The reaction solution was slowly evaporated at room temperature to yield pale pink-coloured blocks of **1**. Yield = 42 mg, 78%, dec. 541 K. FT–IR (ATR cm^{-1}) 2361 (*s*), 2352 (*s*), 2129 (*w*), 1632 (*s*), 1511 (*vs*, $v_{as}NO_2$), 1472 (*s*), 1449 (*s*), 1269 (*vs*, v_sNO_2), 1195 (*s*), 1087 (*s*), 1030 (*vs*, vNO), 806 (*s*), 767 (*vs*), 743 (*vs*), 708 (*s*), 694 (*s*). HRMS (*m/z*) calculated for $C_{28}H_{24}N_{11}O_9Th$ [M −(2HNO$_3$ + NO$_3^-$)] 890.2139; found 890.2139. Elemental analysis calculated (%) for $C_{28}H_{26}N_{14}O_{18}Th$ (1078.63): C 31.18, H 2.43, N 18.18; found C 30.86, H 2.40, N 17.98. Owing to the poor solubility of compound **1** in organic solvents (CHCl$_3$, DMSO and THF), NMR characterization could not be carried out.

The IR spectrum of **1** showed absorptions due to the nitrate ligands at 1511, 1269 and 1030 cm^{-1} (see Fig. S3 in the supporting information). The bands appearing at 1511 and 1269 cm^{-1} correspond to the asymmetric (v_{as}) and symmetric (v_s) NO$_2$ stretching frequencies, respectively, while the band appearing at 1030 cm^{-1} is assigned to $v(NO)$. These values correspond with those of chelating nitrate in [Th(NO$_3$)$_4$·tmu] (tmu = trimethylurea) at 1530, 1278 and 1023 cm^{-1} (Amani &

Tayebee, 2013; Nakamoto, 2008*b*) and are in contrast with those of ionic nitrates (Na and K salts), which appear at 1405–1370 cm^{-1} with ν(NO) only Raman active at 1068–1049 cm^{-1} (Nakamoto, 2008*a*). The high-resolution mass spectrum of **1** showed elimination of two molecules of HNO_3 and loss of the NO_3^- ion, leading to an *m*/*z* value of 820.2139 corresponding to $[Th(NO_3)_3(C_{14}H_{12}N_4)_2]^+$, the formal ionization product of the $[Th(NO_3)_4L_2]$ target (see Fig. S4).

6. Refinement

Crystal data, data collection and refinement details are given in Table 3. C-bound hydrogen atoms were placed in calculated positions (C—H = 0.95–0.99 Å) and refined using a riding model with $U_{iso}(H) = 1.2U_{eq}(C)$. The N-bound H atom H4 was refined with the distance restraint N—H = 0.89±0.02 Å.

Table 3
Experimental details.

Crystal data	
Chemical formula	$(C_{14}H_{13}N_4)_2[Th(NO_3)_6]$
M_r	1078.67
Crystal system, space group	Monoclinic, $P2_1/n$
Temperature (K)	150
a, b, c (Å)	14.5386 (3), 9.3464 (2), 15.4213 (4)
β (°)	117.846 (1)
V (Å^3)	1852.85 (7)
Z	2
Radiation type	Mo $K\alpha$
μ (mm^{-1})	4.12
Crystal size (mm)	$0.09 \times 0.07 \times 0.06$
Data collection	
Diffractometer	Bruker APEXII CCD
Absorption correction	Multi-scan (*SADABS*; Krause *et al.*, 2015)
T_{min}, T_{max}	0.512, 0.746
No. of measured, independent and observed [$I > 2\sigma(I)$] reflections	27737, 4658, 3944
R_{int}	0.023
$(\sin \theta/\lambda)_{max}$ (Å^{-1})	0.673
Refinement	
$R[F^2 > 2\sigma(F^2)]$, $wR(F^2)$, S	0.015, 0.035, 1.05
No. of reflections	4658
No. of parameters	281
No. of restraints	1
H-atom treatment	H atoms treated by a mixture of independent and constrained refinement
$\Delta\rho_{max}$, $\Delta\rho_{min}$ (e Å^{-3})	0.72, −0.33

Computer programs: *APEX4* and *SAINT* (Bruker, 2019), *SHELXT2014/5* (Sheldrick, 2015*a*), *SHELXL2019/3* (Sheldrick, 2015*b*) and *OLEX2* (Dolomanov *et al.*, 2009).

References

Abram, U., Bonfada, E. & Schulz Lang, E. (1999). *Acta Cryst.* C**55**, 1479–1482.
Alcock, N. W., Esperås, S., Bagnall, K. W. & Hsian-Yun, W. (1978). *J. Chem. Soc. Dalton Trans.* pp. 638–646.
Amani, V. & Tayebee, R. (2013). *Synth. React. Inorg. Met.-Org. Nano-Met. Chem.* **43**, 1118–1123.
Aparna, K., Krishnamurthy, S. S. & Nethaji, M. (1995). *J. Chem. Soc. Dalton Trans.* pp. 2991–2997.
Bruker (2019). *APEX4* and *SAINT*. Bruker AXS Inc., Madison, Wisconsin, USA.
Cheng, J. Y., Dong, Y. B., Ma, J. P., Huang, R.-Q. & Smith, M. D. (2005). *Inorg. Chem. Commun.* **8**, 6–8.
Crawford, M. J., Ellern, A., Karaghiosoff, K. & Mayer, P. (2009). *Inorg. Chem.* **48**, 10877–10879.
Dolomanov, O. V., Bourhis, L. J., Gildea, R. J., Howard, J. A. K. & Puschmann, H. (2009). *J. Appl. Cryst.* **42**, 339–341.
Gephart, R. T. III, Williams, N. J., Reibenspies, J. H., De Sousa, A. S. & Hancock, R. D. (2009). *Inorg. Chem.* **48**, 8201–8209.
Goodgame, D. M., Menzer (née Smith), A. M., Menzer, S., White, A. J. & Williams, D. J. (2003). *Inorg. Chim. Acta*, **355**, 314–321.
Groom, C. R., Bruno, I. J., Lightfoot, M. P. & Ward, S. C. (2016). *Acta Cryst.* B**72**, 171–179.
Jin, G. B., Lin, J., Estes, S. L., Skanthakumar, S. & Soderholm, L. (2017). *J. Am. Chem. Soc.* **139**, 18003–18008.
Kelley, S. P., Smetana, V., Emerson, S. D., Mudring, A.-V. & Rogers, R. D. (2020). *Chem. Commun.* **56**, 4232–4235.
Krause, L., Herbst-Irmer, R., Sheldrick, G. M. & Stalke, D. (2015). *J. Appl. Cryst.* **48**, 3–10.
Kumar, N. & Tuck, D. G. (1984). *Can. J. Chem.* **62**, 1701–1704.
Matonic, J. H., Neu, M. P., Enriquez, A. E., Paine, R. T. & Scott, B. L. (2002). *J. Chem. Soc. Dalton Trans.* pp. 2328–2332.
McKinnon, J. J., Jayatilaka, D. & Spackman, M. A. (2007). *Chem. Commun.* 3814–3816.
Mishra, M. K., Choudhary, H., Cordes, D. B., Kelley, S. P. & Rogers, R. D. (2019). *Cryst. Growth Des.* **19**, 3529–3542.
Nakamoto, K. (2008*a*). *Infrared and Raman Spectra of Inorganic and Coordination Compounds*, Part A, 6th ed., pp. 149–354. Hoboken: Wiley.
Nakamoto, K. (2008*b*). *Infrared and Raman Spectra of Inorganic and Coordination Compounds*, Part B, 6th ed., pp. 1–273. Hoboken: Wiley.
Rammo, N. N., Hamid, K. R. & Ibrahim, T. K. (1994). *J. Alloys Compd.* **210**, 319–324.
Rebizant, J., Apostolidis, C., Spirlet, M. R., Andreetti, G. D. & Kanellakopulos, B. (1988). *Acta Cryst.* C**44**, 2098–2101.
Reilly, S. D., Scott, B. L. & Gaunt, A. J. (2012). *Inorg. Chem.* **51**, 9165–9167.
Sheldrick, G. M. (2015*a*). *Acta Cryst.* A**71**, 3–8.
Sheldrick, G. M. (2015*b*). *Acta Cryst.* C**71**, 3–8.
Spackman, M. A. & Jayatilaka, D. (2009). *CrystEngComm*, **11**, 19–32.
Spirlet, M. R., Rebizant, J., Apostolidis, C., Kanellakopulos, B. & Dornberger, E. (1992). *Acta Cryst.* C**48**, 1161–1164.
Surbella, R. G., Ducati, L. C., Autschbach, J., Pellegrini, K. L., McNamara, B. K., Schwantes, J. M. & Cahill, C. L. (2018). *Chem. Commun.* **54**, 12014–12017.
Takao, K., Kazama, H., Ikeda, Y. & Tsushima, S. (2019). *Angew. Chem. Int. Ed.* **58**, 240–243.
Takao, K., März, J., Matsuoka, M., Mashita, T., Kazama, H. & Tsushima, S. (2020). *RSC Adv.* **10**, 6082–6087.
Turner, M. J., Mckinnon, J. J., Wolff, S. K., Grimwood, D. J., Spackman, P. R., Jayatilaka, D. & Spackman, M. A. (2017). *CrystalExplorer17*. The University of Western Australia. https://hirshfeldsurface.net

Urankar, D., Pinter, B., Pevec, A., De Proft, F., Turel, I. & Košmrlj, J. (2010). *Inorg. Chem.* **49**, 4820–4829.

Wang, M., Wang, B., Zheng, P., Wang, W. & Lin, J. (1988). *Acta Cryst.* C**44**, 1913–1916.

Xiao, C.-L., Wang, C.-Z., Yuan, L.-Y., Li, B., He, H., Wang, S., Zhao, Y.-L., Chai, Z.-F. & Shi, W.-Q. (2014). *Inorg. Chem.* **53**, 1712–1720.

Zhang, Y., Yang, S., Yuan, X., Zhao, Y. & Tian, G. (2017). *Chem. Commun.* **53**, 6421–6423.

supporting information

Synthesis, structural studies and Hirshfeld surface analysis of 2-[(4-phenyl-1*H*-1,2,3-triazol-1-yl)methyl]pyridin-1-ium hexakis(nitrato-κ^2O,O')thorate(IV)

Shalini Rangarajan, Sonu Sheokand, Victoria L. Blair, Glen B. Deacon and Maravanji S. Balakrishna

Computing details

2-[(4-Phenyl-1*H*-1,2,3-triazol-1-yl)methyl]pyridin-1-ium hexakis(nitrato-κ^2O,O')thorate(IV)

Crystal data

$(C_{14}H_{13}N_4)_2[Th(NO_3)_6]$	$F(000) = 1052$
$M_r = 1078.67$	$D_x = 1.933$ Mg m^{-3}
Monoclinic, $P2_1/n$	Mo $K\alpha$ radiation, $\lambda = 0.71073$ Å
$a = 14.5386$ (3) Å	Cell parameters from 9957 reflections
$b = 9.3464$ (2) Å	$\theta = 3.9–28.5°$
$c = 15.4213$ (4) Å	$\mu = 4.12$ mm^{-1}
$\beta = 117.846$ (1)°	$T = 150$ K
$V = 1852.85$ (7) Å^3	Block, yellow
$Z = 2$	$0.09 \times 0.07 \times 0.06$ mm

Data collection

Bruker APEXII CCD diffractometer	4658 independent reflections
φ and ω scans	3944 reflections with $I > 2\sigma(I)$
Absorption correction: multi-scan (SADABS; Krause *et al.*, 2015)	$R_{int} = 0.023$
	$\theta_{max} = 28.6°$, $\theta_{min} = 2.7°$
$T_{min} = 0.512$, $T_{max} = 0.746$	$h = -19 \rightarrow 19$
27737 measured reflections	$k = -12 \rightarrow 12$
	$l = -20 \rightarrow 20$

Refinement

Refinement on F^2	Hydrogen site location: mixed
Least-squares matrix: full	H atoms treated by a mixture of independent and constrained refinement
$R[F^2 > 2\sigma(F^2)] = 0.015$	
$wR(F^2) = 0.035$	$w = 1/[\sigma^2(F_o^2) + (0.0109P)^2 + 1.5954P]$
$S = 1.05$	where $P = (F_o^2 + 2F_c^2)/3$
4658 reflections	$(\Delta/\sigma)_{max} < 0.001$
281 parameters	$\Delta\rho_{max} = 0.72$ e Å^{-3}
1 restraint	$\Delta\rho_{min} = -0.33$ e Å^{-3}
Primary atom site location: dual	

Special details

Experimental. A crystal of **1** suitable for X-ray analysis was mounted on a Cryoloop with a drop of Paratone oil and placed in the cold nitrogen stream of the Kryoflex attachment of the Bruker APEX-II CCD diffractometer. The raw data was reduced with *SAINT* V8.40A (Bruker, 2019). The absorption correction was done with *SADABS2016/2* (Bruker, 2016/2). Structural solutions were obtained with SHELXT (Sheldrick, 2015a) and refined using full matrix least-squares against F^2 using SHELXL (Sheldrick, 2015b), in conjunction with the Olex2 (Dolomanov *et al.*, 2009) graphical user interface.

Geometry. All esds (except the esd in the dihedral angle between two l.s. planes) are estimated using the full covariance matrix. The cell esds are taken into account individually in the estimation of esds in distances, angles and torsion angles; correlations between esds in cell parameters are only used when they are defined by crystal symmetry. An approximate (isotropic) treatment of cell esds is used for estimating esds involving l.s. planes.

Fractional atomic coordinates and isotropic or equivalent isotropic displacement parameters (Å²)

	x	y	z	U_{iso}*/U_{eq}
Th1	0.500000	0.500000	0.500000	0.01543 (3)
O3	0.53542 (12)	0.85963 (17)	0.35224 (11)	0.0364 (3)
O8	0.82701 (10)	0.47216 (19)	0.64969 (12)	0.0398 (4)
O7	0.68122 (10)	0.54650 (15)	0.63986 (10)	0.0233 (3)
O4	0.50279 (10)	0.54161 (15)	0.66518 (10)	0.0258 (3)
O9	0.67896 (10)	0.40835 (15)	0.52678 (10)	0.0246 (3)
O1	0.60450 (10)	0.68989 (15)	0.46103 (10)	0.0252 (3)
O2	0.43750 (10)	0.71724 (15)	0.38557 (10)	0.0249 (3)
O5	0.50941 (10)	0.73336 (15)	0.59005 (10)	0.0257 (3)
N5	0.73268 (11)	0.47576 (17)	0.60683 (12)	0.0224 (3)
N3	0.62635 (11)	0.65844 (17)	1.02726 (11)	0.0214 (3)
N4	0.66816 (12)	0.40969 (17)	0.93013 (12)	0.0222 (3)
N1	0.48011 (12)	0.69191 (17)	1.02356 (12)	0.0223 (3)
N2	0.56554 (12)	0.61513 (17)	1.06624 (12)	0.0237 (3)
C9	0.40384 (13)	0.8878 (2)	0.89961 (13)	0.0203 (4)
N6	0.52628 (12)	0.75963 (17)	0.39768 (11)	0.0225 (3)
N7	0.50393 (13)	0.67864 (19)	0.66342 (12)	0.0273 (4)
C10	0.42192 (14)	0.9932 (2)	0.84549 (14)	0.0241 (4)
H10	0.487167	0.996946	0.845381	0.029*
O6	0.49717 (17)	0.7501 (2)	0.72531 (13)	0.0549 (5)
C2	0.58095 (14)	0.7630 (2)	0.96064 (13)	0.0228 (4)
H2	0.608517	0.811145	0.923638	0.027*
C1	0.48597 (13)	0.7850 (2)	0.95776 (13)	0.0198 (3)
C3	0.72825 (14)	0.5927 (2)	1.05898 (14)	0.0267 (4)
H3A	0.741548	0.523286	1.112040	0.032*
H3B	0.782565	0.667624	1.085923	0.032*
C11	0.34551 (15)	1.0927 (2)	0.79172 (14)	0.0266 (4)
H11	0.359140	1.165092	0.756012	0.032*
C14	0.30661 (15)	0.8835 (2)	0.89773 (15)	0.0272 (4)
H14	0.293076	0.812659	0.934452	0.033*
C4	0.67031 (14)	0.3342 (2)	0.85725 (14)	0.0252 (4)
H4A	0.620849	0.260215	0.826229	0.030*
C8	0.73579 (13)	0.51695 (19)	0.97626 (13)	0.0206 (4)
C5	0.74363 (14)	0.3631 (2)	0.82708 (14)	0.0248 (4)

H5	0.746028	0.308832	0.776090	0.030*
C6	0.81363 (15)	0.4723 (2)	0.87221 (15)	0.0258 (4)
H6	0.864548	0.494561	0.852061	0.031*
C7	0.80955 (14)	0.5499 (2)	0.94722 (15)	0.0238 (4)
H7	0.857548	0.625368	0.978375	0.029*
C12	0.24931 (16)	1.0868 (2)	0.78991 (14)	0.0290 (4)
H12	0.196841	1.154400	0.752611	0.035*
C13	0.23014 (16)	0.9816 (2)	0.84285 (16)	0.0317 (5)
H13	0.164176	0.976926	0.841424	0.038*
H4	0.6240 (17)	0.385 (3)	0.9501 (18)	0.043 (7)*

Atomic displacement parameters (Å²)

	U^{11}	U^{22}	U^{33}	U^{12}	U^{13}	U^{23}
Th1	0.01291 (4)	0.01679 (5)	0.01779 (4)	0.00037 (3)	0.00818 (3)	−0.00091 (4)
O3	0.0397 (8)	0.0323 (8)	0.0397 (8)	−0.0027 (7)	0.0206 (7)	0.0131 (7)
O8	0.0141 (6)	0.0579 (11)	0.0414 (9)	0.0031 (6)	0.0081 (6)	−0.0143 (8)
O7	0.0194 (6)	0.0259 (6)	0.0259 (7)	0.0010 (5)	0.0117 (5)	−0.0021 (6)
O4	0.0256 (7)	0.0276 (7)	0.0273 (7)	−0.0011 (5)	0.0151 (6)	−0.0020 (6)
O9	0.0204 (6)	0.0282 (7)	0.0254 (7)	0.0001 (5)	0.0109 (5)	−0.0041 (6)
O1	0.0202 (6)	0.0271 (7)	0.0280 (7)	−0.0004 (5)	0.0110 (5)	0.0012 (6)
O2	0.0198 (6)	0.0263 (7)	0.0290 (7)	0.0002 (5)	0.0116 (5)	0.0006 (6)
O5	0.0254 (7)	0.0249 (7)	0.0282 (7)	0.0002 (5)	0.0136 (6)	−0.0019 (6)
N5	0.0168 (7)	0.0258 (9)	0.0249 (8)	0.0007 (6)	0.0100 (6)	−0.0013 (6)
N3	0.0196 (7)	0.0250 (8)	0.0217 (7)	−0.0016 (6)	0.0113 (6)	−0.0010 (6)
N4	0.0189 (7)	0.0225 (8)	0.0260 (8)	−0.0010 (6)	0.0110 (6)	0.0054 (6)
N1	0.0233 (7)	0.0200 (8)	0.0274 (8)	−0.0044 (6)	0.0150 (7)	−0.0030 (6)
N2	0.0244 (8)	0.0230 (8)	0.0272 (8)	−0.0040 (6)	0.0149 (7)	−0.0021 (7)
C9	0.0209 (8)	0.0203 (9)	0.0211 (9)	−0.0029 (7)	0.0111 (7)	−0.0059 (7)
N6	0.0237 (7)	0.0220 (8)	0.0236 (8)	−0.0012 (6)	0.0126 (6)	−0.0001 (6)
N7	0.0270 (8)	0.0295 (9)	0.0271 (8)	−0.0018 (7)	0.0141 (7)	−0.0073 (7)
C10	0.0224 (8)	0.0267 (9)	0.0250 (9)	−0.0037 (8)	0.0125 (7)	−0.0042 (8)
O6	0.0897 (14)	0.0446 (10)	0.0450 (10)	−0.0058 (10)	0.0439 (10)	−0.0208 (8)
C2	0.0232 (8)	0.0257 (10)	0.0229 (9)	−0.0022 (7)	0.0136 (7)	0.0002 (7)
C1	0.0213 (8)	0.0189 (9)	0.0215 (8)	−0.0052 (7)	0.0121 (7)	−0.0055 (7)
C3	0.0199 (8)	0.0347 (11)	0.0239 (9)	0.0025 (8)	0.0090 (7)	0.0011 (8)
C11	0.0301 (10)	0.0274 (10)	0.0221 (9)	−0.0016 (8)	0.0120 (8)	−0.0006 (8)
C14	0.0260 (9)	0.0295 (10)	0.0327 (10)	0.0007 (8)	0.0193 (8)	0.0022 (8)
C4	0.0229 (9)	0.0201 (9)	0.0280 (10)	−0.0013 (7)	0.0082 (8)	0.0013 (8)
C8	0.0182 (8)	0.0207 (9)	0.0212 (8)	0.0026 (7)	0.0078 (7)	0.0045 (7)
C5	0.0272 (9)	0.0232 (9)	0.0239 (9)	0.0051 (7)	0.0119 (8)	0.0043 (8)
C6	0.0233 (9)	0.0271 (10)	0.0313 (10)	0.0033 (7)	0.0162 (8)	0.0060 (8)
C7	0.0201 (8)	0.0211 (8)	0.0309 (10)	−0.0015 (7)	0.0123 (8)	0.0018 (8)
C12	0.0291 (10)	0.0324 (11)	0.0242 (9)	0.0065 (8)	0.0112 (8)	−0.0004 (8)
C13	0.0259 (9)	0.0383 (12)	0.0363 (11)	0.0046 (8)	0.0190 (8)	0.0006 (9)

Geometric parameters (Å, º)

Th1—O1	2.5830 (13)	N4—H4	0.862 (16)
Th1—O2	2.5621 (14)	C9—C10	1.393 (3)
Th1—O4ⁱ	2.5582 (13)	C9—C1	1.468 (3)
Th1—O4	2.5583 (13)	C9—C14	1.401 (2)
Th1—O5	2.5547 (14)	N7—O6	1.206 (2)
Th1—O7ⁱ	2.5444 (13)	C10—H10	0.9500
Th1—O7	2.5444 (13)	C10—C11	1.388 (3)
Th1—O9ⁱ	2.5827 (12)	C2—H2	0.9500
Th1—O9	2.5827 (12)	C2—C1	1.376 (2)
Th1—O1ⁱ	2.5830 (13)	C3—H3A	0.9900
Th1—O2ⁱ	2.5621 (13)	C3—H3B	0.9900
Th1—O5ⁱ	2.5547 (14)	C3—C8	1.507 (3)
O3—N6	1.212 (2)	C11—H11	0.9500
O8—N5	1.213 (2)	C11—C12	1.387 (3)
O7—N5	1.270 (2)	C14—H14	0.9500
O4—N7	1.281 (2)	C14—C13	1.383 (3)
O9—N5	1.277 (2)	C4—H4A	0.9500
O1—N6	1.279 (2)	C4—C5	1.374 (3)
O2—N6	1.2778 (19)	C8—C7	1.376 (2)
O5—N7	1.278 (2)	C5—H5	0.9500
N1—C1	1.369 (2)	C5—C6	1.379 (3)
N1—N2	1.314 (2)	C6—H6	0.9500
N3—N2	1.343 (2)	C6—C7	1.390 (3)
N3—C2	1.346 (2)	C7—H7	0.9500
N3—C3	1.461 (2)	C12—H12	0.9500
N4—C4	1.340 (3)	C12—C13	1.386 (3)
N4—C8	1.351 (2)	C13—H13	0.9500
O7ⁱ—Th1—O7	180.00 (6)	O8—N5—Th1	177.24 (14)
O7—Th1—O4ⁱ	113.48 (4)	O8—N5—O7	121.59 (16)
O7—Th1—O4	66.52 (4)	O8—N5—O9	122.56 (16)
O7ⁱ—Th1—O4ⁱ	66.52 (4)	O7—N5—Th1	57.08 (8)
O7ⁱ—Th1—O4	113.48 (4)	O7—N5—O9	115.85 (14)
O7ⁱ—Th1—O9	130.23 (4)	O9—N5—Th1	58.86 (8)
O7—Th1—O9ⁱ	130.23 (4)	N2—N3—C2	111.70 (15)
O7ⁱ—Th1—O9ⁱ	49.77 (4)	N2—N3—C3	120.00 (15)
O7—Th1—O9	49.77 (4)	C2—N3—C3	128.30 (16)
O7ⁱ—Th1—O1ⁱ	65.87 (4)	C4—N4—C8	122.43 (16)
O7—Th1—O1ⁱ	114.13 (4)	C4—N4—H4	118.1 (18)
O7ⁱ—Th1—O1	114.13 (4)	C8—N4—H4	119.4 (18)
O7—Th1—O1	65.87 (4)	N2—N1—C1	110.29 (15)
O7ⁱ—Th1—O2	69.99 (4)	N1—N2—N3	106.08 (15)
O7—Th1—O2	110.01 (4)	C10—C9—C1	120.12 (16)
O7—Th1—O2ⁱ	69.99 (4)	C10—C9—C14	118.62 (17)
O7ⁱ—Th1—O2ⁱ	110.01 (4)	C14—C9—C1	121.26 (17)
O7—Th1—O5	67.79 (4)	O3—N6—Th1	176.58 (13)

O7—Th1—O5ⁱ	112.20 (4)	O3—N6—O1	122.44 (15)
O7ⁱ—Th1—O5ⁱ	67.80 (4)	O3—N6—O2	122.05 (16)
O7ⁱ—Th1—O5	112.21 (4)	O1—N6—Th1	58.30 (8)
O4ⁱ—Th1—O4	180.0	O2—N6—Th1	57.35 (9)
O4ⁱ—Th1—O9ⁱ	110.18 (4)	O2—N6—O1	115.51 (15)
O4ⁱ—Th1—O9	69.82 (4)	O4—N7—Th1	57.75 (9)
O4—Th1—O9ⁱ	69.82 (4)	O5—N7—Th1	57.56 (9)
O4—Th1—O9	110.18 (4)	O5—N7—O4	115.19 (15)
O4ⁱ—Th1—O1ⁱ	112.94 (4)	O6—N7—Th1	174.91 (15)
O4—Th1—O1	112.94 (4)	O6—N7—O4	122.04 (18)
O4ⁱ—Th1—O1	67.06 (4)	O6—N7—O5	122.74 (18)
O4—Th1—O1ⁱ	67.06 (4)	C9—C10—H10	119.7
O4—Th1—O2	113.63 (4)	C11—C10—C9	120.61 (17)
O4ⁱ—Th1—O2ⁱ	113.64 (4)	C11—C10—H10	119.7
O4—Th1—O2ⁱ	66.36 (4)	N3—C2—H2	127.5
O4ⁱ—Th1—O2	66.37 (4)	N3—C2—C1	105.06 (16)
O9—Th1—O9ⁱ	180.0	C1—C2—H2	127.5
O9—Th1—O1	66.86 (4)	N1—C1—C9	123.68 (16)
O9ⁱ—Th1—O1	113.14 (4)	N1—C1—C2	106.87 (16)
O9ⁱ—Th1—O1ⁱ	66.86 (4)	C2—C1—C9	129.44 (17)
O9—Th1—O1ⁱ	113.14 (4)	N3—C3—H3A	109.2
O1ⁱ—Th1—O1	180.0	N3—C3—H3B	109.2
O2—Th1—O9ⁱ	67.69 (4)	N3—C3—C8	112.18 (15)
O2—Th1—O9	112.31 (4)	H3A—C3—H3B	107.9
O2ⁱ—Th1—O9ⁱ	112.31 (4)	C8—C3—H3A	109.2
O2ⁱ—Th1—O9	67.69 (4)	C8—C3—H3B	109.2
O2ⁱ—Th1—O1ⁱ	49.70 (4)	C10—C11—H11	119.9
O2ⁱ—Th1—O1	130.30 (4)	C12—C11—C10	120.24 (19)
O2—Th1—O1	49.70 (4)	C12—C11—H11	119.9
O2—Th1—O1ⁱ	130.30 (4)	C9—C14—H14	119.7
O2—Th1—O2ⁱ	180.0	C13—C14—C9	120.56 (19)
O5ⁱ—Th1—O4	130.01 (4)	C13—C14—H14	119.7
O5—Th1—O4	49.99 (4)	N4—C4—H4A	119.8
O5ⁱ—Th1—O4ⁱ	49.99 (4)	N4—C4—C5	120.40 (18)
O5—Th1—O4ⁱ	130.01 (4)	C5—C4—H4A	119.8
O5ⁱ—Th1—O9ⁱ	66.29 (4)	N4—C8—C3	118.14 (16)
O5ⁱ—Th1—O9	66.29 (4)	N4—C8—C7	118.73 (17)
O5—Th1—O9	113.71 (4)	C7—C8—C3	123.11 (17)
O5—Th1—O9ⁱ	113.71 (4)	C4—C5—H5	120.6
O5ⁱ—Th1—O1ⁱ	69.63 (4)	C4—C5—C6	118.76 (19)
O5—Th1—O1ⁱ	110.37 (4)	C6—C5—H5	120.6
O5ⁱ—Th1—O1	110.37 (4)	C5—C6—H6	120.1
O5—Th1—O1	69.63 (4)	C5—C6—C7	119.86 (18)
O5ⁱ—Th1—O2ⁱ	67.02 (4)	C7—C6—H6	120.1
O5—Th1—O2	67.02 (4)	C8—C7—C6	119.81 (18)
O5—Th1—O2ⁱ	112.98 (4)	C8—C7—H7	120.1
O5ⁱ—Th1—O2	112.98 (4)	C6—C7—H7	120.1
O5—Th1—O5ⁱ	180.0	C11—C12—H12	120.2

N5—O7—Th1	98.16 (10)	C13—C12—C11	119.64 (19)
N7—O4—Th1	97.20 (11)	C13—C12—H12	120.2
N5—O9—Th1	96.11 (9)	C14—C13—C12	120.31 (18)
N6—O1—Th1	96.79 (10)	C14—C13—H13	119.8
N6—O2—Th1	97.82 (10)	C12—C13—H13	119.8
N7—O5—Th1	97.47 (11)		
Th1—O7—N5—O8	177.14 (16)	C9—C14—C13—C12	−0.8 (3)
Th1—O7—N5—O9	−3.46 (16)	C10—C9—C1—N1	170.29 (17)
Th1—O4—N7—O5	−3.92 (16)	C10—C9—C1—C2	−8.1 (3)
Th1—O4—N7—O6	173.99 (18)	C10—C9—C14—C13	0.3 (3)
Th1—O9—N5—O8	−177.22 (17)	C10—C11—C12—C13	0.6 (3)
Th1—O9—N5—O7	3.39 (16)	C2—N3—N2—N1	0.5 (2)
Th1—O1—N6—O3	−176.06 (16)	C2—N3—C3—C8	−62.5 (3)
Th1—O1—N6—O2	4.18 (15)	C1—N1—N2—N3	−0.4 (2)
Th1—O2—N6—O3	176.02 (15)	C1—C9—C10—C11	−178.78 (17)
Th1—O2—N6—O1	−4.23 (16)	C1—C9—C14—C13	179.74 (19)
Th1—O5—N7—O4	3.92 (16)	C3—N3—N2—N1	−179.63 (16)
Th1—O5—N7—O6	−173.96 (18)	C3—N3—C2—C1	179.72 (18)
N3—C2—C1—N1	0.2 (2)	C3—C8—C7—C6	178.06 (17)
N3—C2—C1—C9	178.82 (18)	C11—C12—C13—C14	0.4 (3)
N3—C3—C8—N4	−59.3 (2)	C14—C9—C10—C11	0.7 (3)
N3—C3—C8—C7	122.20 (19)	C14—C9—C1—N1	−9.2 (3)
N4—C4—C5—C6	−0.9 (3)	C14—C9—C1—C2	172.4 (2)
N4—C8—C7—C6	−0.5 (3)	C4—N4—C8—C3	−178.54 (16)
N2—N3—C2—C1	−0.4 (2)	C4—N4—C8—C7	0.0 (3)
N2—N3—C3—C8	117.63 (18)	C4—C5—C6—C7	0.5 (3)
N2—N1—C1—C9	−178.62 (16)	C8—N4—C4—C5	0.7 (3)
N2—N1—C1—C2	0.1 (2)	C5—C6—C7—C8	0.2 (3)
C9—C10—C11—C12	−1.1 (3)		

Symmetry code: (i) −x+1, −y+1, −z+1.

Hydrogen-bond geometry (Å, º)

*Cg*1, *Cg*2 and *Cg*3 are the centroids of rings C9–C14, N1–N3/C1/C2, and N4/C4–C8, respectively.

D—H···*A*	*D*—H	H···*A*	*D*···*A*	*D*—H···*A*
N4—H4···N1[ii]	0.86 (3)	1.88 (3)	2.738 (3)	170 (3)
C2—H2···O8[iii]	0.95	2.33	3.261 (3)	168
C7—H7···O5[iv]	0.95	2.46	3.379 (3)	164
C13—H13···O4[v]	0.95	2.46	3.377 (3)	163
N4—H4···N2[ii]	0.86	2.65 (3)	3.432 (3)	151
C10—H10···O8[iii]	0.95	2.68	3.621 (3)	173
C5—H5···O2[i]	0.95	2.68	3.191 (2)	114
C7—H7···O2[iii]	0.95	2.67	3.279 (3)	123
C7—H7···O9[iii]	0.95	2.69	3.369 (2)	129

Symmetry codes: (i) −x+1, −y+1, −z+1; (ii) −x+1, −y+1, −z+2; (iii) −x+3/2, y+1/2, −z+3/2; (iv) x−1/2, −y+1/2, z−1/2; (v) −x+1/2, y+1/2, −z+3/2.